Journal of Alloys and Compounds 628 (2015) 293–297

Contents lists available at ScienceDirect

Journal of Alloys and Compounds

journal homepage: www.elsevier.com/locate/jalcom

Band alignments at interface of Cu_2ZnSnS_4/ZnO heterojunction: An X-ray photoelectron spectroscopy and first-principles study

Gang Yang [a], Yong-Feng Li [a,b], Bin Yao [a,b,*], Zhan-Hui Ding [b], Rui Deng [c], Jie-Ming Qin [c], Fang Fang [d], Xuan Fang [d], Zhi-Peng Wei [d], Lei Liu [e]

[a] Key Laboratory of Physics and Technology for Advanced Batteries (Ministry of Education), College of Physics, Jilin University, Changchun 130012, PR China
[b] State Key Lab of Superhard Materials and College of Physics, Jilin University, Changchun 130023, PR China
[c] School of Materials Science and Engineering, Changchun University of Science and Technology, Changchun 130022, PR China
[d] State Key Laboratory on High-Power Semiconductor Lasers, Changchun University of Science and Technology, 7186 Wei-Xing Road, Changchun 130022, PR China
[e] State Key Laboratory of Luminescence and Applications, Changchun Institute of Optics, Fine Mechanics and Physics, Chinese Academy of Sciences, No. 3888 Dongnanhu Road, Changchun 130033, PR China

ARTICLE INFO

Article history:
Received 26 July 2014
Received in revised form 5 December 2014
Accepted 6 December 2014
Available online 31 December 2014

Keywords:
Cu_2ZnSnS_4
ZnO
Heterojunction
Band alignment
X-ray photoelectron spectroscopy
First-principles calculation

ABSTRACT

The band alignments at the interface of Cu_2ZnSnS_4 (CZTS)/ZnO heterojunction were determined by X-ray photoelectron spectroscopy. Core levels of S2p and O1s were used to align the valence-band offset (VBO). The VBO was determined to be 1.78 ± 0.10 eV, and the conduction-band offset (CBO) was deduced to be 0.09 ± 0.10 eV, implying that the CZTS/ZnO heterojunction has a type-I band alignment. Furthermore, first-principles calculations based on hybrid functional method also indicate that the CZTS/ZnO interface has a type-I band alignment, well supporting our experimental results.

1. Introduction

In the past two decades, thin film solar cells have attracted much attention of many researchers [1–9]. Kesterite Cu_2ZnSnS_4 (CZTS) is a promising photovoltaic material for high efficiency thin film solar cells. It has a direct and suitable bandgap of ~1.5 eV and a high absorption coefficient (>10^4 cm^{-1}) in the visible region, which are suitable for solar cells [10–15]. Comparing with $Cu(In,Ga)Se_2$ (CIGS), all the constituent elements of CZTS are relatively non-toxic and abundant in the nature [16,17]. CZTS thin films have been prepared by various approaches such as non-vacuum methods: electro-deposition [18], sol–gel [19], nanoparticle routes [20] and vacuum methods: sputtering [21], and pulsed-laser deposition [22].

Up to now, $Cu_2ZnSn(S_xSe_{1-x})_4$ (CZTSSe)/CdS heterojunction solar cells have achieved the efficiency over 12% [23]. Considered that Cd is a highly toxic element, a more environmental friendly buffer layer should be found to replace CdS. The candidate must be transparent to the solar spectrum and its conduction-band minimum (CBM) should align well with that of the CZTS absorber. ZnO is a wide-bandgap n-type semiconductor material (the bandgap: 3.37 eV at room temperature), consists of abundant and nontoxic elements [24–27]. Using ZnO as the buffer layer instead of CdS (the band gap: 2.42 eV at room temperature [28]) will guarantee a higher light transmittance in the shorter wavelength regions, thus ZnO is expected to be a good substitute. But up to now, the efficiencies have been reported for CZTSSe devices utilizing ZnO as the buffer material are just 4.3% and 5.2% [29,30], much lower than those of using CdS as the buffer layer [31].

It is important to determine the band alignments at the interface for achieving high efficiency cells. There is now a general consensus that valence-band offset (VBO) and conduction-band offset (CBO) are two of the crucial parameters which determine the electronic behavior of the heterojunction interface [32]. If the CBM of the n-type buffer (window) layer is higher than that of the p-type absorber layer (type-I heterojunction), the CBO forms a barrier for the photo-excited electrons crossing the interface, the photocurrent will be considerably reduced if the barrier's height is too large. However, when CBM of the buffer layer is lower than that of the

* Corresponding author at: Key Laboratory of Physics and Technology for Advanced Batteries (Ministry of Education), College of Physics, Jilin University, Changchun 130012, PR China.
E-mail addresses: liyongfeng@jlu.edu.cn (Y.-F. Li), binyao@jlu.edu.cn (B. Yao).

http://dx.doi.org/10.1016/j.jallcom.2014.12.174
0925-8388/

absorber layer (type-II heterojunction), which is equivalent to an interface band gap reduction, though the barrier against photon generated electrons is not formed, an increased recombination rate for majority carriers at the interface may cause a relative low open circuit voltage (V_{OC}) and a poor fill factor (FF) that influence the quality of solar cells directly. In view of that, we should fabricate solar cells with a type-I interface and also have a small barrier height, namely a very small ΔE_C. Recently both experiment results and first-principles studies demonstrate CdS forms type-II heterojunctions with both CZTSSe and CZTS [33–35]. But the precise values of band offsets for CZTS/ZnO heterojunction were few reported. Bao and Ichimura [36] calculated the band offsets at the CZTS/ZnO interface from first-principles calculations, they declared ΔE_V is in the range of 0.8–1.3 eV, and the CBM of CZTS is predicted to be lower than that of ZnO. However, Barkhouse et al. [37] investigated the band alignments of the CZTSSe/ZnO using femtosecond ultraviolet photoemission and photo-voltage spectroscopy, they indicated that the ΔE_V is 2.1 eV, and the corresponding ΔE_C is almost null, but they did not give the results for pure sulfide CZTS.

In this paper, we investigated the band alignments at the CZTS/ZnO interface by combining X-ray photoelectron spectroscopy (XPS) and first-principles calculations. We found a type-I band alignment at the interface of the CZTS/ZnO heterojunction with an ideal CBO value.

2. Experimental and first-principles calculations details

We prepared three samples (CZTS, ZnO, CZTS/ZnO bilayer) to determine the band alignments of the CZTS/ZnO heterojunction. The deposition of the CZTS films on cleaned Soda-Lime glass (SLG) substrates were conducted in a RF magnetron sputtering system with a single CZTS target of 60 mm in diameter and 3 mm in thickness. Prior to the films growth, the chamber was evacuated to 7.5×10^{-4} Pa and the substrates were heated to 500 °C. Ar (99.99%) with a flow of 30 SCCM was introduced as working gas during the deposition, the sputtering pressure was controlled to be 0.1 Pa and the growth time was 120 min. ZnO films were obtained using the same method except the working pressure was 1 Pa. For the CZTS/ZnO heterojunction, a thin ZnO layer with a thickness of ~5 nm (minimizes band bending in the buffer layer and hence uncertainty in the VBO measurement) was deposited on the thick CZTS film, for 20 s using the same growth conditions as the thick ZnO film. It should be noted that a thicker ZnO layer is necessary in an actual device. Fig. 1 shows a cross-sectional SEM picture of a typical CZTS/ZnO heterojunction with a thickness of 200 nm, in which the sputtering time of ZnO layer is 12 min. All the films were performed XPS test by ESCALAB 250 XPS instrument with an Al Kα ($h\nu$ = 1486.6 eV) X-ray radiation source which had been carefully calibrated on work function and Fermi energy level. The XPS spectra were calibrated by the C1s peak (284.6 eV). An ultraviolet–visible spectrophotometer was used to record the optical absorption spectra of these films.

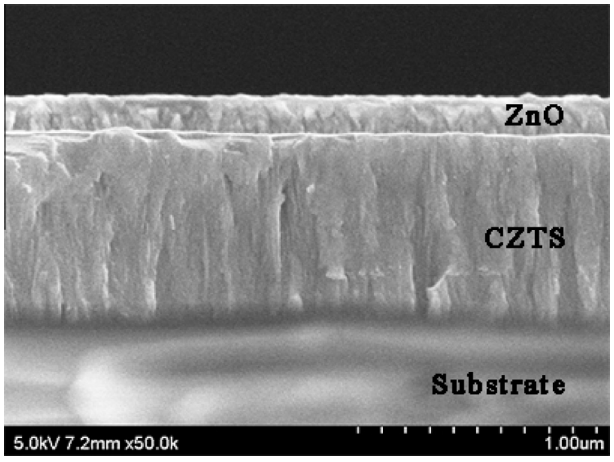

Fig. 1. Cross-sectional SEM picture of a typical CZTS/ZnO heterjunction.

The calculation method of heterojunction band offset had been discussed in detail by Wei and Zunger [38]. For our case, the VBO of CZTS/ZnO heterojunction can be calculated by the following formula:

$$\Delta E_V = \Delta E_{CL} + \left(E_{S2p}^{CZTS} - E_{VBM}^{CZTS}\right) - \left(E_{O1s}^{ZnO} - E_{VBM}^{ZnO}\right) \quad (1)$$

In which $\Delta E_{CL} = E_{O1s}^{ZnO} - E_{S2p}^{CZTS}$ is the energy difference between S2p and O1s core levels (CLs) in the CZTS/ZnO heterojunction, $E_{S2p}^{CZTS} - E_{VBM}^{CZTS}$ is the energy difference between S2p and valence-band maximum (VBM) in the CZTS film, and $E_{O1s}^{ZnO} - E_{VBM}^{ZnO}$ is the energy difference between O1s and VBM in the ZnO film.

To better understand the band alignments from XPS measurements, the first-principles calculations were performed using the plane-wave projector-augmented-wave (PAW) method [39,40] applying the Heyd–Scuseria–Ernzerhof (HSE) hybrid functional [41] as implemented in the VASP code [42,43]. We constructed three structures: bulk CZTS, ZnO, and CZTS/ZnO superlattices for calculating the VBO of the interface. It should be noted that the zinc-blende (ZB) ZnO is adopted to match the crystal structure of CZTS. We expect the results from the ZB ZnO are also applicable for the wurtzite (WZ) ones, because some previous reports have indicated that some properties in ZB and WZ are quite similar [44–46]. The CZTS/ZnO interface vertical [0 0 1] direction was constructed. The lattice constant along the heterointerface was fixed to the average of those of CZTS and ZnO. In order to discuss the effects of strain on ΔE_V, we also adopted the two limiting cases of lattice constraint conditions ($a = a_{ZnO}$ and $a = a_{CZTS}$). Here we adopted the average electrostatic potential (AEP) as the core-level to align the valence-band [47]. To calculate the CBO, the experimental bandgaps were used, because the first-principles usually underestimate them, even though the hybrid functional method is used here.

3. Results and discussion

3.1. Experimental results

We first measured the energy difference between core levels (CLs) in the separated CZTS and ZnO film. As depicted in the

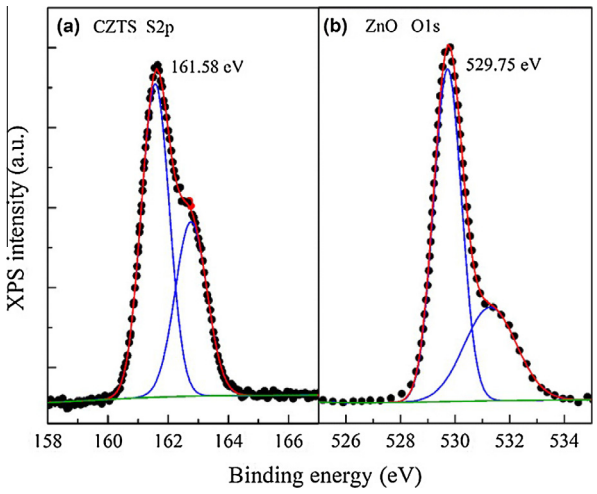

Fig. 2. (a) CL of S2p recorded on CZTS sample and (b) CL of O1s recorded on ZnO sample.

Fig. 2, the values are 161.58 ± 0.05 eV and 529.75 ± 0.05 eV for $S2p_{3/2}$ and O1s respectively. Then, we measured the energy difference between two characteristic CLs for the CZTS/ZnO heterojunction sample, as shown in Fig. 3. Compared with the spectra recorded on the separated CZTS and ZnO samples, the O1s peak in the CZTS/ZnO heterojunction shifts 0.14 eV to a binding energy of 529.89 ± 0.05 eV, and the $S2p_{3/2}$ peak shifts to 161.60 ± 0.05 eV. The shifts can be ascribe to band bending or change of space charge at the interface if no chemical shifts take place during the deposition process [48]. The peaks located at about 531.51 eV were assigned to the adsorbed oxygen.

Fig. 4 shows the VB spectra of the thick CZTS and ZnO films. The values of VBM can be deduced by linearly extrapolating the low-binding-energy edge of the valence band and intersecting it with the base lines to account for the instrument resolution induced tail [49]. The obtained VBM values of CZTS and ZnO are 0.46 ± 0.10 eV and 2.12 ± 0.10 eV, respectively. The parameters obtained from above were summarized in Table 1 for clarity. Substituting the experimental values (Table 1) into Eq. (1), the resulting VBO value is 1.78 ± 0.10 eV for CZTS/ZnO heterojunction, which is larger than the results from first principles calculations [36]. In order to determine the CBO of the heterojunction, the bandgaps of the CZTS and ZnO films were determined by the optical absorption spectra, as shown in Fig. 5. The bandgaps (E_g) were determined to be 1.50 eV for CZTS and 3.37 eV for ZnO. The CBO can be calculated by the formula $\Delta E_C = E_g^{ZnO} - E_g^{CZTS} - \Delta E_V$. As a result, the CBO is deduced to be 0.09 eV. The schematic diagram of band alignments of the heterojunction based on the measured results is shown in Fig. 6, indicating a type-I alignment at the CZTS/ZnO interface.

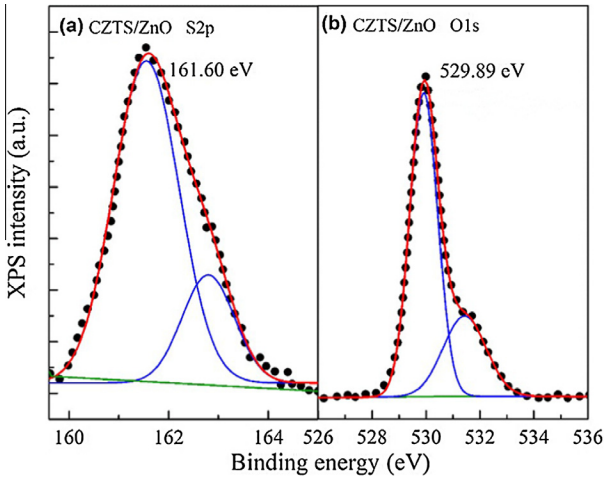

Fig. 3. (a) CL of S2p recorded on CZTS/ZnO sample and (b) CL of O1s recorded on CZTS/ZnO sample.

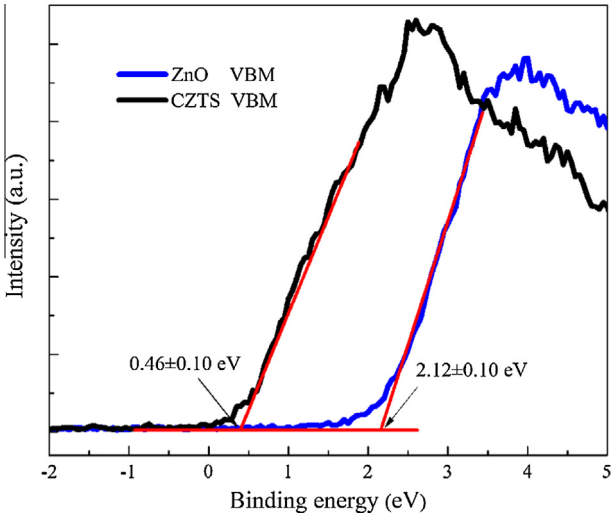

Fig. 4. The valence-band edge (VBE) spectra for CZTS and ZnO samples. The VBM values are determined by liner extrapolation of the leading edge to the base line.

Table 1
Peak positions of CLs and VBM positions used to calculate the VBO of p-CZTS /n-ZnO heterojunction.

Sample	Region	Binding energy (eV)
ZnO	O 1s	529.75 ± 0.05
	VBM	2.12 ± 0.10
CZTS	S $2p_{3/2}$	161.58 ± 0.05
	VBM	0.46 ± 0.10
CZTS/ZnO	O 1s	529.89 ± 0.05
	S $2p_{3/2}$	161.60 ± 0.05

3.2. First-principles calculations results

To better understand the band alignments at the interface of CZTS/ZnO heterojunction, we calculated electronic structure and VBO of CZTS/ZnO based on the first-principles method. The detailed calculation method and configuration are described in the Section 2. To calculate the VBO of CZTS/ZnO interface, we constructed CZTS/ZnO superlattices, as shown in Fig. 7(a). The calculated VBO is 1.80 eV for the CZTS/ZnO interface when the lattice constant $a = a_{AVE}$. To discuss the effects of strain, we also calculated ΔE_V using the same method for the two limiting cases of lattice constraint conditions ($a = a_{ZnO}$ and $a = a_{CZTS}$). The ΔE_V was determined to be 2.23 eV and 1.49 eV for $a = a_{ZnO}$ and $a = a_{CZTS}$ respectively. The ΔE_V decreases with increasing lattice constant. According to Eq. (1), the ΔE_V is determined by three terms: ΔE_{CL}, energy differences between the core level and VBM for ZnO and CZTS. We found that the change of ΔE_V with lattice constant is derived from the following: (i) for $a = a_{ZnO}$, this would be due to the interaction between the atomic orbitals enhanced when CZTS under compressive strain, which cause the increase of the energy difference between *Ev* and the core level, (ii) for $a = a_{CZTS}$, the energy difference between *Ev* and the core level decreases when ZnO is under tensile strain, but the difference between core level energies enlarged for the CZTS/ZnO heterojunction. In the actual CZTS/ZnO heterojunction, since the lattice mismatch is extremely

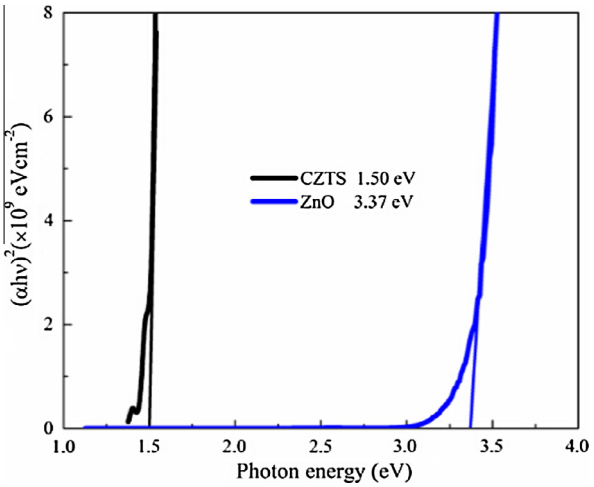

Fig. 5. Optical absorption spectra of CZTS and ZnO films grown on SLG substrates.

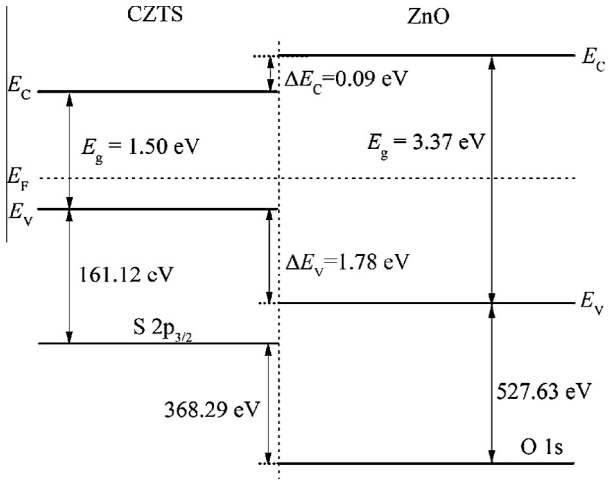

Fig. 6. Schematic diagram of type-I band alignment of a CZTS/ZnO heterojunction determined by XPS.

large, the strain will be mostly relaxed by misfit dislocation at the interface, so that each layer is almost strain-free. Herein, we used the results of the lattice constraint condition $a = a_{AVE}$ to align the band offset. This lattice constraint condition has been used in many other investigations and proved to agree with the experimental results well [50,51]. Actually, our calculated ΔE_V using the lattice constraint condition $a = a_{AVE}$ is also well consistent with XPS results. The experimental bandgaps of CZTS and ZnO are used to determine the CBO at the CZTS/ZnO interface, and the calculated CBO is 0.07 eV. The schematic diagram of the calculated band alignments of CZTS/ZnO heterojunction is shown in Fig. 7(b), also indicating a type-I alignment. The calculated results well support our experimental results.

It should be noted that, in our previous work [35], ΔE_V (CZTS/ZnO) can be deduced to be 2.92 eV and 2.13 eV for the XPS and calculation results from ΔE_V (CZTS/ZnO) = ΔE_V (CZTS/CdS) + ΔE_V (CdS/ZnO) according to the transitivity rule, which are larger than we obtained here. There seems a discrepancy between our present and previous work. As we have discussed above, the difference of lattice constant will significantly influence the ΔE_V. Some researchers also reported that ΔE_V is different as deformation potential are taken into account or not [52,38]. In our band offset calculations, we used average lattice constant as lattice constraint condition to construct the superlattices. The lattice constant for each heterointerface is different, i.e. the lattice constant is 5.64 Å for CZTS/CdS, 5.22 Å for CdS/ZnO and 5.05 Å for CZTS/ZnO. In this case, the calculated band offsets are not unstained "natural" ones. Therefore, the transitivity rule is not suitable for the large strained band offsets or the violation of the transitivity rule is derived from the large strain due to large lattice mismatch in band offset calculations. On the other hand, in our experiments, large lattice mismatch will produce a large amount of defects, such as dislocation, to relax the strain. Fermi level position is determined by the concentration of these defects. The ΔE_V is strongly dependent on Fermi level position. Therefore, we ascribed the violation of transitivity rule in the experiments to different lattice mismatch which results in different Fermi level. In summary, lattice mismatch plays a key role in leading to the violation of transitivity rule for both first-principles calculations and experiments.

3.3. Discussion

It can be seen in both experimental results and first principles calculations that the valence band edge of CZTS is higher than that for ZnO, with the conduction band edge of ZnO is higher than that of CZTS, leading to a type-I heterojunction with a negligible CBO, which is an ideal band structure for a solar cell with an n-type win-

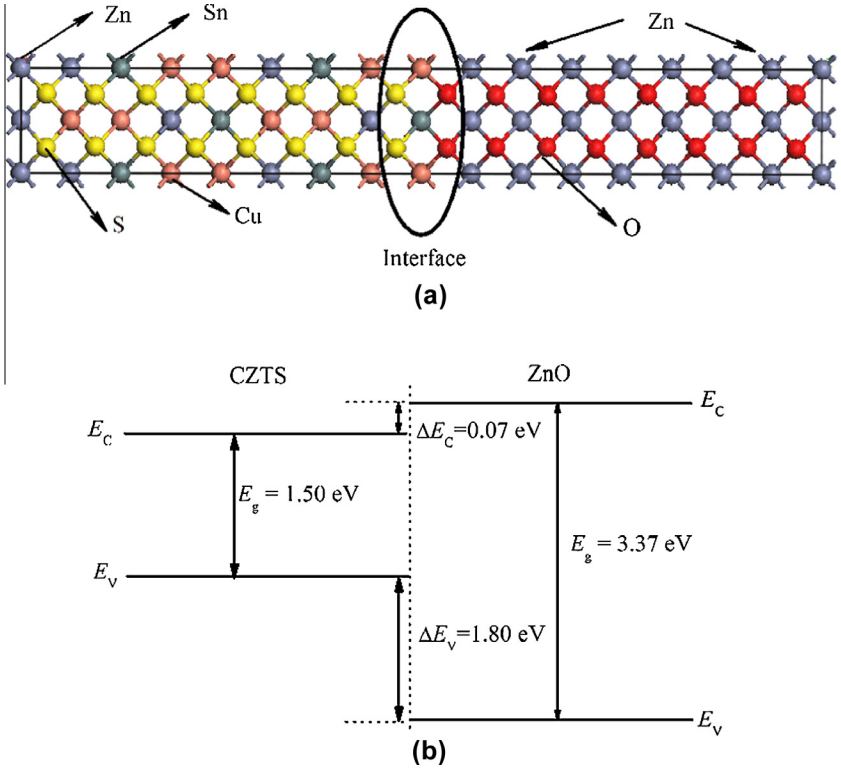

Fig. 7. (a) Supercell of CZTS/ZnO superlattices and (b) schematic diagram of type-I band alignment of a CZTS/ZnO heterojunction determined by hybrid functional first-principles calculations.

dow layer and a p-type absorber layer [53]. On the one hand, the cliff will not form when ΔE_C is positive, the V_{OC} as well as the relative quantum efficiency at the short-wavelength regions may increase obviously, this is corresponding to the experimental results [29], in which the V_{OC} is 650 meV for CZTS/ZnO solar cells and 620 meV for CZTS/CdS solar cells. On the other hand, if the ΔE_C is too large, a notch formed will block the electron transfer from the CZTS layer to the ZnO layer, the photo-current will reduce considerably, but this can be neglected when conduction band alignment is almost flat. Therefore, we can infer that ZnO may be a suitable nontoxic buffer layer material for high efficiency CZTS solar cells in the future.

4. Conclusions

We used XPS combined with first principles calculations based on hybrid functional method to decide the band alignments of the CZTS/ZnO heterojunction. Both of them shown that the CZTS/ZnO heterojunction is a type-I heterojunction with a positive VBO about 1.78 eV and a negligible positive CBO. The conduction band alignment obtained suggests that ZnO can be an attractive Cd-free buffer candidate for CZTS based solar cells.

Acknowledgments

This work is supported by the National Natural Science Foundation of China under Grant Nos. 10874178, 11074093, 61205038 and 11274135, Specialized Research Fund for the Doctoral Program of Higher Education under Grant No. 20130061130011, Ph.D. Programs Foundation of Ministry of Education of China under Grant No. 20120061120011, Natural Science Foundation of Jilin Province under Grant No. 201115013, and National Found for Fostering Talents of Basic Science under Grant No. J1103202. This work was also supported by High Performance Computing Center of Jilin University, China.

References

[1] G. Altamura, L. Grenet, C. Bougerol, E. Robin, D. Kohen, H. Fournier, A. Brioude, S. Perraud, H. Mariette, J. Alloys Compd. 588 (2014) 310–315.
[2] T. Ericson, J.J. Scragg, T. Kubart, T. Törndahl, C. Platzer-Björkman, Thin Solid Films 535 (2013) 22–26.
[3] S.A. Vanalakar, G.L. Agawane, S.W. Shin, M.P. Suryawanshi, K.V. Gurav, K.S. Jeon, P.S. Patil, C.W. Jeong, J.Y. Kim, J.H. Kim, J. Alloys Compd. 619 (2015) 109–121.
[4] Z.C. Holman, S. De Wolf, C. Ballif, Light Sci. Appl. 2 (2013) e106.
[5] J.J. Scragg, T. Ericson, X. Fontané, V. Izquierdo-Roca, A. Pérez-Rodríguez, T. Kubart, M. Edoff, C. Platzer-Björkman, Prog. Photovoltaics Res. Appl. 22 (2014) 10–17.
[6] Y.-M. Choi, Y.-I. Lee, S. Kim, Y.-H. Choa, J. Alloys Compd. 615 (2014) 496–500.
[7] Y.-H. Su, Y.-F. Ke, S.-L. Cai, Q.-Y. Yao, Light Sci. Appl. 1 (2012) e14.
[8] E. Aydin, M. Sankir, N.D. Sankir, J. Alloys Compd. 615 (2014) 461–468.
[9] X. Chen, B. Jia, Y. Zhang, M. Gu, Light Sci. Appl. 2 (2013) e92.
[10] F. Aslan, A. Tumbul, J. Alloys Compd. 612 (2014) 1–4.
[11] M. Guc, R. Caballero, K.G. Lisunov, N. López, E. Arushanov, J.M. Merino, M. León, J. Alloys Compd. 596 (2014) 140–144.
[12] X. Zeng, K.F. Tai, T. Zhang, C.W.J. Ho, X. Chen, A. Huan, T.C. Sum, L.H. Wong, Sol. Energy Mater. Sol. Cells 124 (2014) 55–60.
[13] A.I. Inamdar, S. Lee, K.-Y. Jeon, C.H. Lee, S.M. Pawar, R.S. Kalubarme, C.J. Park, H. Im, W. Jung, H. Kim, Sol. Energy 91 (2013) 196–203.
[14] S. Ahmed, K.B. Reuter, O. Gunawan, L. Guo, L.T. Romankiw, H. Deligianni, Adv. Energy Mater. 2 (2012) 253–259.
[15] H. Wang, Int. J. Photoenergy 2011 (2011) 1–10.
[16] B. Shin, O. Gunawan, Y. Zhu, N.A. Bojarczuk, S.J. Chey, S. Guha, Prog. Photovoltaics Res. Appl. 21 (2013) 72–76.
[17] S. Jung, J. Gwak, J.H. Yun, S. Ahn, D. Nam, H. Cheong, S. Ahn, A. Cho, K. Shin, K. Yoon, Thin Solid Films 535 (2013) 52–56.
[18] Y. Li, T. Yuan, L. Jiang, Z. Su, F. Liu, J. Alloys Compd. 610 (2014) 331–336.
[19] Z.-Y. Xiao, Y.-F. Li, B. Yao, R. Deng, Z.-H. Ding, T. Wu, G. Yang, C.-R. Li, Z.-Y. Dong, L. Liu, L.-G. Zhang, H.-F. Zhao, J. Appl. Phys. 114 (2013) 183506.
[20] W. Huang, Q. Li, Y. Chen, Y. Xia, H. Huang, C. Dun, Y. Li, D.L. Carroll, Sol. Energy Mater. Sol. Cells 127 (2014) 188–192.
[21] C. Yan, J. Chen, F. Liu, N. Song, H. Cui, B.K. Ng, J.A. Stride, X. Hao, J. Alloys Compd. 610 (2014) 486–491.
[22] A.V. Moholkar, S.S. Shinde, A.R. Babar, K.-U. Sim, H.K. Lee, K.Y. Rajpure, P.S. Patil, C.H. Bhosale, J.H. Kim, J. Alloys Compd. 509 (2011) 7439–7446.
[23] M.T. Winkler, W. Wang, O. Gunawan, H.J. Hovel, T.K. Todorov, D.B. Mitzi, Energy Environ. Sci. 7 (2014) 1029.
[24] N. Izyumskaya, V. Avrutin, Ü. Özgür, Y.I. Alivov, H. Morkoç, Phys. Status Solidi (b) 244 (2007) 1439–1450.
[25] D.D. Wang, G.Z. Xing, F. Yan, Y.S. Yan, S. Li, Appl. Phys. Lett. 104 (2014) 022412.
[26] G.Z. Xing, D.D. Wang, C.J. Cheng, M. He, S. Li, T. Wu, Appl. Phys. Lett. 103 (2013) 022402.
[27] G.Z. Xing, Y.H. Lu, Y.F. Tian, J.B. Yi, C.C. Lim, Y.F. Li, G.P. Li, D.D. Wang, B. Yao, J. Ding, Y.P. Feng, T. Wu, AIP Adv. 1 (2011) 022152.
[28] A.I. Oliva, O. Solis-Canto, R. Castro-Rodriguez, P. Quintana, Thin Solid Films 391 (2001) 28–35.
[29] M.T. Htay, Y. Hashimoto, N. Momose, K. Sasaki, H. Ishiguchi, S. Igarashi, K. Sakurai, K. Ito, Jpn. J. Appl. Phys. 50 (2011) 032301.
[30] H. Katagiri, K. Jimbo, M. Tahara, H. Araki, K. Oishi, Mrs., The influence of the composition ratio on CZTS-based thin film solar cells, in: A. Yamada, C. Heske, M.A. Contreras, M. Igalson, S.J.C. Irvine (Eds.), Thin-Film Compound Semiconductor Voltaics-2009, 2010, pp. 125–136.
[31] G. Brammertz, M. Buffière, S. Oueslati, H. ElAnzeery, K. Ben Messaoud, S. Sahayaraj, C. Köble, M. Meuris, J. Poortmans, Appl. Phys. Lett. 103 (2013) 163904.
[32] A. Santoni, F. Biccari, C. Malerba, M. Valentini, R. Chierchia, A. Mittiga, J. Phys. D: Appl. Phys. 46 (2013) 175101.
[33] R. Haight, A. Barkhouse, O. Gunawan, B. Shin, M. Copel, M. Hopstaken, D.B. Mitzi, Appl. Phys. Lett. 98 (2011) 253502.
[34] J. Li, Q. Du, W. Liu, G. Jiang, X. Feng, W. Zhang, J. Zhu, C. Zhu, Electron. Mater. Lett. 8 (2012) 365–367.
[35] Z.-Y. Dong, Y.-F. Li, B. Yao, Z.-H. Ding, G. Yang, R. Deng, X. Fang, Z.-P. Wei, L. Liu, J. Phys. D: Appl. Phys. 47 (2014) 075304.
[36] W. Bao, M. Ichimura, Jpn. J. Appl. Phys. 52 (2013) 061203.
[37] D.A.R. Barkhouse, R. Haight, N. Sakai, H. Hiroi, H. Sugimoto, D.B. Mitzi, Appl. Phys. Lett. 100 (2012) 193904.
[38] S.-H. Wei, A. Zunger, Appl. Phys. Lett. 72 (1998) 2011.
[39] G. Kresse, D. Joubert, Phys. Rev. B 59 (1999) 1758–1775.
[40] P.E. Blöchl, Phys. Rev. B 50 (1994) 17953–17979.
[41] J. Heyd, G.E. Scuseria, M. Ernzerhof, J. Chem. Phys. 124 (2006) 219906.
[42] G. Kresse, J. Furthmüller, Phys. Rev. B 54 (1996) 11169–11186.
[43] G. Kresse, J. Furthmüller, Comput. Mater. Sci. 6 (1996) 15–50.
[44] Y.Q. Gai, B. Yao, Z.P. Wei, Y.F. Li, Y.M. Lu, D.Z. Shen, J.Y. Zhang, D.X. Zhao, X.W. Fan, J. Li, J.-B. Xia, Appl. Phys. Lett. 92 (2008) 062110.
[45] C.-Y. Yeh, S.-H. Wei, A. Zunger, Phys. Rev. B 50 (1994) 2715–2718.
[46] S. Limpijumnong, S.B. Zhang, S.-H. Wei, C.H. Park, Phys. Rev. Lett. 92 (2004) 155504.
[47] M. Peressi, N. Binggeli, A. Baldereschi, J. Phys. D: Appl. Phys. 31 (1998) 1273.
[48] A.R. Kumarasinghe, W.R. Flavell, A.G. Thomas, A.K. Mallick, D. Tsoutsou, C. Chatwin, S. Rayner, P. Kirkham, S. Warren, S. Patel, P. Christian, P. O'Brien, M. Gratzel, R. Hengerer, J. Chem. Phys. 127 (2007) 114703.
[49] C.J. Dong, W.X. Yu, M. Xu, J.J. Cao, C. Chen, W.W. Yu, Y.D. Wang, J. Appl. Phys. 110 (2011) 073712.
[50] W. Bao, M. Ichimura, Jpn. J. Appl. Phys. 51 (2012) 10NC31.
[51] W. Bao, M. Ichimura, Int. J. Photoenergy 2012 (2012) 1–5.
[52] Y.-H. Li, A. Walsh, S. Chen, W.-J. Yin, J.-H. Yang, J. Li, J.L.F. Da Silva, X.G. Gong, S.-H. Wei, Appl. Phys. Lett. 94 (2009) 212109.
[53] D. Kieven, A. Grimm, I. Lauermann, T. Rissom, R. Klenk, Appl. Phys. Lett. 96 (2010) 262101.